

Aberystwyth University

Negative muons reveal the economic chaos of Rome's AD 68/9 Civil Wars

Green, G. A.; Ishida, K.; Domoney, K.; Agoro, T.; Hillier, A. D.

Published in:

Archaeological and Anthropological Sciences

DOI:

[10.1007/s12520-022-01631-1](https://doi.org/10.1007/s12520-022-01631-1)

Publication date:

2022

Citation for published version (APA):

Green, G. A., Ishida, K., Domoney, K., Agoro, T., & Hillier, A. D. (2022). Negative muons reveal the economic chaos of Rome's AD 68/9 Civil Wars. *Archaeological and Anthropological Sciences*, 14(9), [165].
<https://doi.org/10.1007/s12520-022-01631-1>

Document License

CC BY

General rights

Copyright and moral rights for the publications made accessible in the Aberystwyth Research Portal (the Institutional Repository) are retained by the authors and/or other copyright owners and it is a condition of accessing publications that users recognise and abide by the legal requirements associated with these rights.

- Users may download and print one copy of any publication from the Aberystwyth Research Portal for the purpose of private study or research.
- You may not further distribute the material or use it for any profit-making activity or commercial gain
- You may freely distribute the URL identifying the publication in the Aberystwyth Research Portal

Take down policy

If you believe that this document breaches copyright please contact us providing details, and we will remove access to the work immediately and investigate your claim.

tel: +44 1970 62 2400
email: is@aber.ac.uk



Negative muons reveal the economic chaos of Rome's AD 68/9 Civil Wars

G. A. Green^{1,2} · K. Ishida³ · K. Domoney¹ · T. Agoro^{4,5} · A. D. Hillier⁵

Received: 26 May 2022 / Accepted: 12 July 2022
© The Author(s) 2022

Abstract

During the AD 68/9 Civil Wars, Galba, Otho, Vitellius and then Vespasian fought for — and gained — control of the Roman Empire. Our textual sources suggest that this was a period of serious and sustained disruption. However, existing analyses of gold coinages produced in AD 68/9 show only a minor reduction in the purity of the gold coinage. Using X-ray fluorescence, we identify a number of heavily debased gold coins issued during the AD 68/9 Civil Wars, and many slightly debased coins issued in their immediate aftermath. We then confirm the interior composition of these coins totally non-destructively using muonic X-ray emission spectroscopy, thus eliminating hypothetical problems of ‘surface enrichment’ or compositional differences between ‘surface’ and ‘core’. Here we show that heavily debased Civil War gold coinages were indeed produced; that copper was used to debase Roman gold coins during this time, c. 185 years earlier than first shown; and that slightly debased gold coins were regularly issued in the years immediately after the Civil Wars. The metallurgical evidence from the gold coinage now allows us to show that the AD 68/9 Civil Wars caused significant and sustained disruption to the Roman economic system. More broadly, we have shown that muonic X-ray emission spectroscopy is a powerful tool for generating important archaeological conclusions from high-value cultural heritage objects that simply cannot be destructively analysed, but need to have their interior compositions sampled.

Keywords Muons · Roman · Gold · Coins · Non-destructive · Purity

Introduction

With the suicide of Nero on the 9th of June AD 68, the Roman Empire was launched into a series of civil wars that lasted until the accession of Vespasian on the 21st of December AD 69. Even then, Vespasian faced a revolt in Gaul (France) in AD 70 that required most of the year to quell. During AD 68 and AD 69, Galba, Otho, Vitellius and

then Vespasian were declared as emperor; leading this time to be dubbed the ‘Year of the Four Emperors’.

Our ancient authors — Suetonius, Plutarch, Cassius Dio and Tacitus — make it very clear that this was a period of bloody civil wars and acute fiscal crisis. Furthermore, analyses of the silver coinage show that the purity of the *denarius* dropped from c. 90 to c. 80% under Otho and that this lower purity was retained by Vitellius and Vespasian (Butcher et al. 2014). Yet, existing metallurgical analyses of the gold coinages produced by these emperors (Bocciarelli et al. 2017) show little more than a ‘wobble’ in the purity: a drop to c. 98–99% pure. Hardly evidence for sustained, significant disruption. However, initial X-ray fluorescence (XRF) analyses of 44 gold coins — *aurei* — held by the Ashmolean Museum suggest that this collection may be able to radically alter the current thinking. Several heavily debased issues were identified from the AD 68/9 Civil Wars and a sustained period of slight debasement was observed during the first few years of Vespasian's reign. The major problem when constructing such narratives about gold objects solely with XRF is that the data collected are

✉ G. A. Green
george.green@ashmus.ox.ac.uk

¹ Ashmolean Museum, University of Oxford, Beaumont Street, Oxford OX1 2PH, UK

² Lincoln College, Turl Street, Oxford OX1 3DR, UK

³ RIKEN Nishina Center, RIKEN, Wako, Saitama 351-0198, Japan

⁴ Department of Mathematics and Physics, Aberystwyth University, Penglais SY23 3FL, UK

⁵ ISIS Neutron and Muon Facility, STFC Rutherford Appleton Laboratory, Didcot OX11 0QX, UK

only from the first < 10 microns: the lingering ‘what if’ of differences between the ‘surface’ and ‘core’ of an object undermines any conclusions drawn.

For Roman silver coinages, it is sometimes possible to undertake destructive drilling to sample the metal at the centre of the coin. Roman gold coins are, however, much rarer and much more valuable. This means that permission for such destructive work on Roman gold is routinely not granted by cultural heritage institutions. As such, a non-destructive technique able to analyse the metal at the very centre of these coins was needed to validate the pattern produced by the XRF analyses.

To do this, we have employed a cutting-edge technique called muonic X-ray emission spectroscopy (μ XES). We, and others, have previously shown that μ XES produces congruent results with XRF on the surfaces of Roman gold coins and is capable of producing accurate results when analysing the centres of gold objects (Green et al. 2021; Ninomiya et al. 2015). The technique works by controlling the momentum of the muons and firing them at the sample, they then pass through the material and are eventually captured by the atoms well beneath the surface of the object. In our case, the muons penetrated c. 0.4 mm into *aurei* that were c. 1 mm thick. The energy of the resulting muonic X-rays from the capture indicates the element from which it came, enabling us to determine sub-surface elemental composition totally non-destructively.

With a combination of XRF and μ XES, we seek to answer three key questions:

What was the true scale of the debasements undertaken during the AD 68/9 Civil Wars and their aftermath?

Did deliberate surface enrichment or the inclusion of other metals, whether deliberately or accidentally, occur during the production of *aurei* at this time?

Can these metallurgical analyses aid us in understanding the true scale of the disruption caused by the ‘Year of the Four Emperors’ to the Roman fiscal system?

Broadly speaking, by answering these questions, we hope to further show that the μ XES technique is a powerful tool that has the potential to radically alter our understanding of both individual archaeological objects and the broad archaeological narratives we create from them.

Results

The gold content of the 44 *aurei* analysed by XRF are presented in Fig. 1. These were issued between AD 65 and AD 77. Of these coins, 12 had their composition validated by μ XES: these are denoted by solid markers on Fig. 1 and are detailed in a truncated data table (Table 1). A full data table can be found in the supplementary material.

During the AD 68/9 Civil Wars, the purity of the gold coinage becomes more erratic, dropping below 99% pure,

Fig. 1 Gold content of 44 *aurei* as determined by XRF. Coins solely analysed by XRF are denoted by hollow markers, and coins checked for significant surface enrichment with μ XES are denoted by filled markers

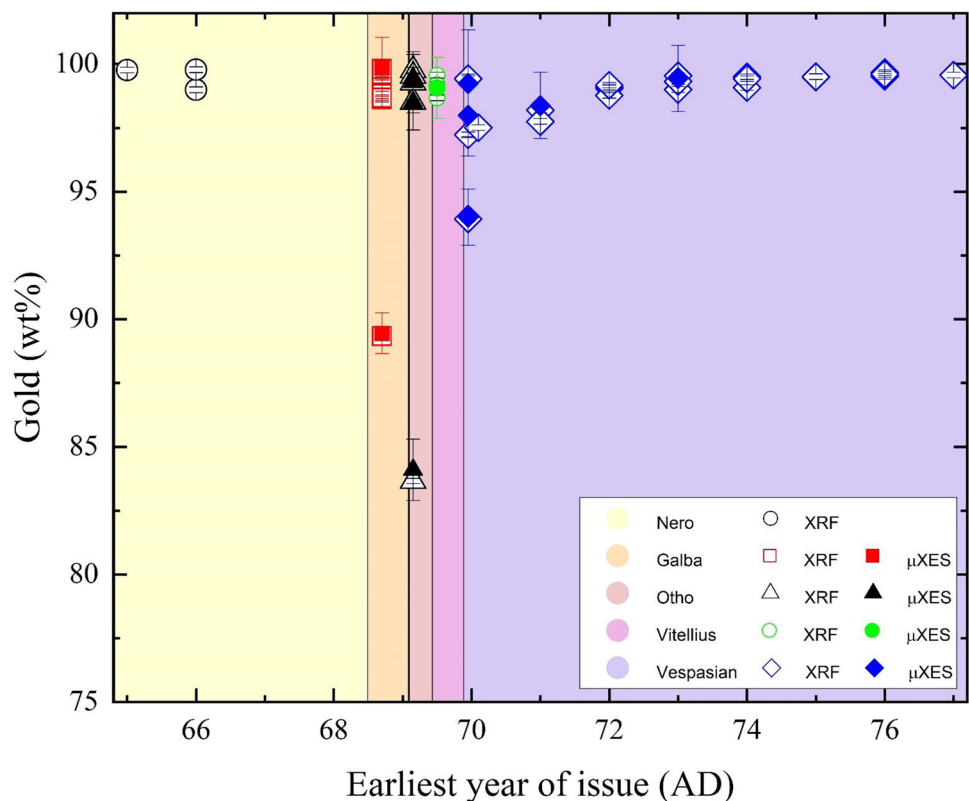


Table 1 A truncated data table detailing the XRF and μ XES results of all the aurei analysed by μ XES. Asterisks (*) denote below detection. Coins mentioned explicitly in the ‘Discussion’ section are also included here. All data and errors can be found in the supplementary material

#	Emperor	Date (AD)	Mint	XRF Au (%)	\bar{x} Au error (\pm)	XRF Ag (%)	XRF Cu (%)	μ XES Au (%)	μ XES Ag (%)	μ XES Cu (%)	μ XES error (\pm)
9	Galba	68–9	Tarraco	99.59	0.14	0.41	*	99.8	0.2	*	0.8–1.2
11	Galba	68–9	Tarraco	89.33	0.14	4.92	5.75	89.4	4.8	5.8	0.4–0.8
13	Otho	69	Rome	99.75	0.14	0.25	*	N/A	N/A	N/A	N/A
14	Otho	69	Rome	99.53	0.14	0.47	*	99.5	0.5	*	0.6–0.9
15	Otho	69	Rome	98.52	0.14	1.14	0.34	98.5	1.5	*	0.8–1.1
16	Otho	69	Rome	83.66	0.33	10.94	5.40	84.1	9.4	6.5	0.4–1.2
17	Otho	69	Rome	99.27	0.14	0.65	0.12	99.3	0.7	*	0.8–1.2
20	Vitellius	69	Rome	99.56	0.14	0.44	*	99.1	0.9	*	0.5–1.2
22	Vespasian	69–70	Tarraco	97.23	0.14	2.77	*	98.0	2.0	*	0.7–1.6
23	Vespasian	69–70	Rome	99.42	0.14	0.58	*	99.2	0.8	*	0.8–2.1
24	Vespasian	69–79	Uncertain	93.92	0.14	4.02	2.06	94.0	3.9	2.1	0.3–1.1
26	Vespasian	71	Lugdunum	98.19	0.14	1.81	*	N/A	N/A	N/A	N/A
27	Vespasian	71	Lugdunum	97.75	0.14	1.95	0.31	98.4	1.6	*	0.5–1.3
33	Vespasian	73	Rome	99.54	0.14	0.46	*	99.4	0.6	*	0.5–1.3

with a few coins struck heavily debased. From AD 70, the purity of the gold coinage seems to become more consistent, but this is achieved at a lower purity. It is not until AD 73/4 that *aurei* are struck consistently at ‘full’ purity again, i.e. > 99% gold.

μ XES has enabled us to confirm the internal composition of key coins totally non-destructively. The internal fabric of the three most impure *aurei* (Table 1, #11, 16, 24) really were debased with both silver and copper to the degree suggested by XRF. For all three coins, there is excellent agreement between the gold measurements by XRF and μ XES. Coin #16 contains the only slight disagreement (c. 1–1.5%) between the silver and copper measurements, but given the margin of error for the μ XES measurements, this should not be over-interpreted. Copper leaching from the surface to the archaeological environment is a potential explanation, but this should have also caused a greater concentration of gold at the ‘surface’ relative to the ‘core’ — this is not the case here. As such, inherent error is the preferred explanation. Crucially, the higher-purity *aurei* sampled all show no evidence of being surface enriched and hiding major debasements beneath the surface that XRF cannot detect. There is, overall, excellent agreement between the gold purity determined by XRF and μ XES. In all, there is no compelling evidence for the existence of surface enrichment in the coins analysed.

Discussion

To some extent, the analyses performed here are in broad agreement with the previous analyses of gold coinages produced during the ‘Year of the Four Emperors’. Like Bocciarelli et al. (Bocciarelli et al. 2017), we have detected intermittent debasements of between one and two percentage points during the AD 68/9 Civil Wars. This, however, significantly understates the instability caused by the ‘Year of the Four Emperors’. The Ashmolean collection seems to contain a number of much more heavily debased issues, which perhaps reveal the true extent of the disruption to the Roman monetary system. Of the six *aurei* of Galba analysed, one was heavily debased at only 89.3% pure (XRF \pm 0.14, μ XES 89.4% \pm 0.8); of the five *aurei* of Otho analysed, one was heavily debased at only 83.7% pure (XRF \pm 0.33, μ XES 84.1% \pm 1.2); and of the three *aurei* of Vespasian with an earliest issue date of AD 69 analysed, two were debased at 93.9% (XRF \pm 0.14, μ XES 94.0% \pm 1.1) and 97.2% pure (XRF \pm 0.14, μ XES 98.0% \pm 1.6). We also analysed coins produced in the immediate aftermath of the Civil Wars once Vespasian had taken control of the Empire. Broadly speaking, it seems to have taken a few years for Vespasian to restore the purity of the *aureus*: *aurei* issued in AD 70 and AD 71 cluster at around 97% pure, but by AD 74, they seem

to be clustering at approximately 99% pure again (Fig. 1). The purities of all the noticeably debased coins, as well as a sub-sample of high-purity coins, were validated with μ XES (Table 1), so we know that these particularly low figures are not a result of surface enrichment or hypothetical diagenetic alterations.

Of the 21 coins analysed with an earliest issue date of AD 68 or AD 69, seven contained greater than 1% silver. In three of these cases, the silver concentration remained under 1.5%, with the overall purity of these three coins ranging from 98.4% to 98.7% pure ($XRF \pm 0.14$). As such, 17 of the 21 coins analysed that were issued in AD 68/9 contained less than 1.5% silver and their purities ranged from 98.4% to 99.7% ($XRF \pm 0.14$) (Fig. 1). These 17 examples exhibit the same pattern identified by Bocciarelli et al. (Bocciarelli et al. 2017) of slight, intermittent debasements during the AD 68/9 Civil Wars. These relatively low concentrations of silver were most probably the result of not quite fully parting all of the silver from the gold used to strike *aurei*. The parting of silver from gold requires the use of a cementation technique which has to be run multiple times to achieve full purity gold (Blet-Lemarquand et al. 2017; Notton 1974). Not running this process to completion is not only quicker and less resource intensive, but also leaves a greater mass of metal to be struck into coinage. The inclusion of such small quantities of silver in these gold coinages would have had a negligible effect on state finances: these 17 coins had a mean purity of 99%, and Bocciarelli et al. (Bocciarelli et al. 2017) give mean purities for the *aurei* of Galba, Otho and Vitellius from Rome of between 99.2% and 99.5% and from provincial mints of between 98.4% and 99.7%. This all gives the impression that these various competing emperors ultimately had quite tight control over the purity of their gold coinages, with shorter processing times occasionally being favoured over slightly higher purity gold. This does not speak to excessive strain on state finances nor to the disruption of key operations. The heavily debased coins we have identified here, however, do.

Under Galba, an 89.3% pure ($XRF \pm 0.14$, μ XES 89.4% ± 0.8) *aureus* containing 4.9% silver ($XRF \pm 0.14$, μ XES 4.8% ± 0.8) was struck at Tarraco in Spain; under Otho, an 83.7% pure ($XRF \pm 0.33$, μ XES 84.1% ± 1.2) *aureus* containing 10.9% ($XRF \pm 0.20$, μ XES 9.4% ± 1.2) silver was struck in Rome; and under Vespasian, a 93.9% ($XRF \pm 0.14$, μ XES 94.0% ± 1.1) and a 97.2% ($XRF \pm 0.14$, μ XES 98.0% ± 1.6) *aureus* containing 4.0% ($XRF \pm 0.06$, μ XES 3.9% ± 1.1) and 2.8% ($XRF \pm 0.06$, μ XES 2.0% ± 1.6) silver respectively were issued, the latter being struck in Tarraco. These coins are not the product of slightly shorter cementation processes, but either

a result of the deliberate addition of silver into the gold stock or the termination of the parting process significantly before completion. If totally deliberate, then this represents clear evidence of the true scale of the fiscal crisis suffered by these various competing emperors during the immediate Civil War period. Perhaps the decision made was to stretch the gold stocks by heavily debasing only some coins, rather than employing a smaller debasement across all *aurei* issued. If the inclusion of these high concentrations of silver was accidental, then this must surely be indicative of serious disruption to the normal functioning of minting operations — such errors are vanishingly rare in the previous 100 years of *aureus* production (Callu et al. 1985; Caley 1952; Blet-Lemarquand et al. 2015). Even in the latter case, the decision to allow *aurei* that were of low or uncertain purities out into circulation reflects the unique fiscal strains of the time: simply put, our various Emperors needed gold coinage to meet their obligations and could not afford to have that particular gold stock rejected and reprocessed.

The acquiescence of these particularly low purity examples can perhaps be seen in the addition of copper. Copper debasements are much rarer in this period, but three can be detected. We can be more confident that when we see a few percentage points of copper in the gold coinage that this had been deliberately added into the stock of gold. Native gold normally contains under 1% copper (Guerra and Calligaro 2004; Raub 1995), and sequestering gold from smelted ores involved separating the gold-silver mix from associated base metals (Bachman 1995; Healy 1979). Furthermore, we only see copper concentrations at the percentage level when there is above 4% silver in the coin. This is the approximate area where colorimetric methods, like a touchstone, would probably be able to detect that the gold was impure (Oddy 1986). As such, it would seem that copper was deliberately added into gold with a high silver content in order to darken the colour of the alloy and make it appear to be a much ‘more gold’ gold. Compositional analyses have shown that gold objects with elevated copper contents (as high as 10%) became increasingly typical in New Kingdom Egypt, suggesting the deliberate and regular addition of copper at this time to darken the colour of the objects (Ogden 2000). This is probably what happened during the production of the three heavily debased *aurei* of Galba, Otho and Vespasian (Table 1, #11, 16, 24). These contain c. 4–11% silver alongside c. 2–6% copper. The addition of copper into Roman gold coinage had previously only been observed during the debasements of the mid-third century (Callu et al. 1985). As μ XES enables us to be totally confident

that there are significant concentrations of copper in the fabric of these coins, we are able to bring back the earliest use of this particular debasement technique in Roman gold coins the Romans by 185 years to the AD 68/9 Civil Wars.

Further interesting is that the purity of the above coins was not considered to be an aberration, but rather something that could be ‘fixed’ by changing the visual properties of the coin. This is perhaps indicative of the financial strains of the immediate Civil War period on these various claimants: while the low purity was clearly not ideal or deliberately aimed for, the need to stretch the gold stocks and issue gold coinage quickly overrode the need to produce a consistently pure gold coinage. At least in the short term. Nevertheless, this reveals that the debasements in this period were not always coherent or tightly controlled, with a practical need to produce more gold coinage clearly taking priority during the Civil Wars. The epitome of this can be seen across the four ‘RIC2 9’ type *aurei* issued under Otho (Table 1, #13–16). These were all struck in Rome between the 15th of January and the 16th of April AD 69. Two were essentially full purity (Table 1, #13, 14), one was slightly debased at 98.5% pure (XRF ± 0.14 , $\mu\text{XES } 98.5\% \pm 1.1$) and the fourth was the heavily debased, 83.7% pure (XRF ± 0.33 , $\mu\text{XES } 84.1\% \pm 1.2$) coin detailed above. Otho’s regime was clearly technologically capable of producing a full purity coinage, there does not appear to have been a coherent decision to systematically debase this series of coinage either slightly or seriously, and so the relatively chaotic production of this coinage must be seen as a reflection of the chaos of the time.

With all this in mind, the metallurgy of the gold coinage produced during the AD 68/9 Civil Wars now provides a much more complementary picture with our textual sources. Suetonius (*Galba*, 12; *Vitellius* 13, 14, 17; *Vespasian*, 16) and Cassius Dio (LXIV.2–3; LXV.5.3; LXVI.2.5, 14.4–5) accuse Galba, Vitellius and Vespasian of being greedy, money-grabbing or parsimonious while emperor. Tacitus (*Histories* I.5, 49; II.62) repeats such comments against Galba and Vitellius. Both Otho (Suetonius, *Otho*, 5; Plutarch, *Life of Galba*, 21) and Vitellius (Suetonius, *Vitellius*, 7, 14; Plutarch, *Life of Otho*, 4; Cassius Dio, LXV.2) are recorded as having considerable personal debts. Galba is accused by all our authors of not paying out the donatives he promised the troops (Suetonius, *Galba*, 16, 17; Cassius Dio, LXIV.3–25; Plutarch, *Life of Galba*, 22, 23; Tacitus, *Histories*, I.5, 25, 41); Vitellius, according to Tacitus (*Histories*, II.69, 94), did not have the funds to pay out to the army what he had promised and attempted to reduce troop numbers; and Vespasian is presented as reluctant to pay further

donatives to the army by both Suetonius (*Vespasian*, 8) and Tacitus (*Histories*, II.82). All our emperors seem to incur extraordinary expenses either to secure their position or to feed the vices of their inner circle. Galba seems to have made frequent gifts to, or allowed rapacious behaviour from, his friends and freedmen (Suetonius, *Galba*, 15; Plutarch, *Life of Galba*, 16; Tacitus, *Histories*, I.7); Otho is recorded as buying influence, loyalty and supporters (Suetonius, *Otho*, 4–7; Plutarch, *Life of Galba*, 20, *Life of Otho*, 1, 3; Cassius Dio, LXIV.8; Tacitus, *Histories*, I.23–4, 46, 79); Vitellius apparently spent lavishly on his vices (Suetonius, *Vitellius*, 13, Cassius Dio, LXV.2–4; Tacitus, *Histories*, II.71, 94–5); and Vespasian undertook a large building program from the outset of his reign (Suetonius, *Vespasian*, 9; Cassius Dio, LXVI.10; Tacitus, *Histories*, IV.53). Finally, we see these various emperors attempting to increase their revenues. Galba attempts recoup 90% of the value of the gifts that Nero had given out (Suetonius, *Galba*, 15; Plutarch, *Life of Galba*, 16; Cassius Dio, LXIV.3; Tacitus, *Histories*, I.20); Vitellius’ troops were apparently particularly rapacious (Plutarch, *Life of Otho*, 6; Tacitus, *Histories*, II.56); and Vitellius himself allegedly oversaw the confiscation of wealth from his opponents (Suetonius, *Vitellius*, 14; Tacitus, *Histories*, II.92). Then, under Vespasian, the senate accepted a loan of 60 million sesterces shortly after his victory (Tacitus, *Histories*, IV.47); and on his accession, he re-implemented taxes remitted by Galba, created new ones and increased the tribute due from the provinces (Suetonius, *Vespasian*, 6; Cassius Dio, LXVI.8).

Of course, our ancient authors were not accountants and nor did they intend to be. The salacious *specifics* of these accusations of parsimony, vice, greed, rapaciousness, indebtedness and profligacy should probably be treated with absolute suspicion — these all form part of an established pejorative canon employed by Roman writers over hundreds of years. What is interesting is that all our major authors feel comfortable firing the entire canon of pejorative fiscal commentary at our competing emperors during this period. We can infer from this that our authors perceived this period to be one of such fiscal instability that it could be safely used as the narrative backdrop for a variety of moralising devices, motifs and themes revolving around fiscal inadequacy. With this in mind, we can now see the metallurgy of the gold coinage in much closer agreement with the broad narrative favoured by our textual sources.

One of the more mundane claims made by Plutarch (*Life of Galba*, 20) was that when Galba revolted, Otho was one of the first provincial governors to join his cause and brought with him silver and gold ‘drinking cups and

tables' that were to be melted down into coinage. If this is not an invention of Plutarch — the relatively banality may lend it credibility compared to the more moralising claims detailed above — then both Galba and Otho are implicated in the recycling of precious metal objects into coins. Such objects would have been of uncertain purity and so their use may well have contributed to the erratic purity of the gold coinage in this period. Indeed, it is not unthinkable that in a time of crisis that our competing emperors would simply melt down any precious metal they could get their hands on, rather than waiting for the products of more established supply chains. Equally, as outlined above, it is also understandable why such gold may have not have been parted or refined properly during the Civil War period.

Once Vespasian had control of the empire, we would expect to see a degree of consistency and control restored, even if the stock of gold still had to be stretched. This can perhaps be seen in the AD 71 issues from Lugdunum where both *aurei* seem have c. 2% of silver either deliberately added into, or allowed to remain in, the coin. Although a more consistent purity is achieved, *aurei* over the next few years still drop below 99% pure, suggesting continued fiscal instability in the immediate aftermath of the AD 68/9 Civil Wars. This may help explain why Vespasian retained a reputation for avarice throughout his reign (Suetonius, *Vespasian*, 23; Cassius Dio, LXVI.14). Regardless, this continued slight impurity gives some indication of the level of economic disruption caused by the 'Year of the Four Emperors'.

Generally speaking, however, between AD 70 and AD 74, there is a relatively smooth, gradual return to producing full purity *aurei*. By the latter half of his reign, Vespasian clearly had control of the fineness of his *aurei*: from AD 74 onwards, none of his *aurei* analysed dropped under 99% pure. Vespasian restoring metallurgical stability and securing the position of Flavian dynasty is an important event to observe. His son Titus finally defeated the Jewish Revolt in AD 73, sacking the Second Temple in Jerusalem in AD 70, which ultimately catalysed the development of the Rabbinic Judaism that we recognise today; under Vespasian and Titus, the Colosseum in Rome was built and then inaugurated in AD 80/1; and the Arch of Titus was built under Domitian that featured vanishingly rare contemporary renderings of the religious artefacts taken from the Second Temple — the menorah on the arch was used as the model for the menorah on the emblem of the modern state of Israel. The accession of the Flavians after the AD 68/9 Civil Wars was, then, a momentous turning point in human history that can still be felt today.

Conclusion

We have shown that both pure, slightly debased and heavily debased *aurei* were produced at Rome, Tarraco and Lugdunum in this period. With μ XES, we have shown, totally non-destructively, that the broad pattern shown by XRF on the 'surfaces' of the gold coins can be seen in the 'core' of the objects. Thus, we have eliminated the possibility that the range of purities observed was the product of surface enrichment or contamination.

The debasements identified were all relatively short lived and should probably be seen as a product of the acute instability brought on by the various Civil Wars these claimants for the throne were fighting. We have to assume that the fiscal inadequacy of the claimants played some part in these debasements, but we cannot rule out that our competing emperors did not always have access to the time, resources and skilled labour needed to produce a consistently high-purity gold coinage. The level of debasement seen is not insignificant. *Aurei* that are only 80 to 95% pure are not produced again until the 'Third Century Crisis', which should give some idea of the true scale of the disruption caused by the AD 68/69 Civil Wars. Our textual sources are in good agreement that this was a period of notable fiscal instability, and our analyses now provide metallurgical evidence to support such readings of the texts. Furthermore, thanks to μ XES we are able to confidently state that the three most heavily debased *aurei* contained c. 2–6% copper. The earliest use of copper as a debasement technique in gold coinage under the Roman Empire can now be securely dated to the AD 68/9 Civil Wars. Finally, it seems that a few years recovery time was required before the state was able to start producing *aurei* at full purity again.

We have, therefore, demonstrated a new archaeological narrative that the AD 68/9 Civil Wars caused sustained, significant economic instability. The 'Year of the Four Emperors', then, is not just an historical bridge between two successful dynasties, but a significantly disruptive event in its own right.

Materials and methods

X-ray fluorescence

The XRF analyses were performed using an Oxford Instruments 'X-MET8000' handheld energy dispersive X-ray fluorescence unit with a voltage of 40 kV, a current of 8 μ A and a 1000 μ m aluminium filter. The unit contains

a rhodium target X-ray tube and a 25 mm² high resolution silicon-drift detector. This particular analyser comes factory-loaded with fundamental parameters (FP) that are specific to various applications. All analyses here were performed using the pre-loaded 'Precious Metals FP' calibration setting. External standards of known quantities of gold, silver and copper were also used throughout the analysis. On each coin, three separate c. 5 mm × 5 mm spots were analysed — two on one face of the coin, and one spot on the other — with the results averaged. The flattest parts of the coins were chosen for analysis, as irregularly shaped surfaces can affect the accuracy of the results produced (Blakelock 2016; Geil and Thorne 2014). The handheld unit was docked into a benchtop stand, and the built-in camera was used to select the spots. Each spot was analysed for 30 s, totalling 90 s per coin. Quantitative results were extracted using the standard software provided with the unit. These results were then manually compared with the spectra to check for anomalies — sum peaks, escape peaks, diffraction errors and surface contamination (Tanaka et al. 2017) — that the standard software did not identify or account for. In terms of overall analytical protocol with an X-MET8000, similarities can be seen in both Simsek Franci's (Simsek Franci 2020) analysis of ceramics and Baker et al.'s (Baker et al. 2018) analysis of Byzantine coins.

In short, the technique itself works by firing an X-ray beam at the sample. This displaces electrons from the inner orbital shells of the atoms in the sampled area, as the energy of the X-ray is greater than the binding energy that holds the electrons in their correct orbits. This creates an electron vacancy leaving the particle in an excited state. Relaxation of the excited state occurs through a cascade of outer electrons falling into lower orbitals. As this occurs, X-rays are emitted with energies corresponding to the energy difference between electron orbitals. This energy of this X-ray is characteristic of the element it is emitted from. The intensities of these characteristic X-rays are proportional to the concentration of that element within the sample and can, therefore, be used to quantify the concentrations of the elements present in the sample. The brevity of this explanation is deliberate as dissections of XRF have been undertaken on a number of occasions (Karydas 2007; Hall 1961; Cowell 1998; Grieken and Markowicz 2001). However, one aspect of the technique worth drawing attention to is that it only returns data from the first few micrometres of the object analysed (Blakelock 2016; Hall 1961; Grieken and Markowicz 2001) — if the surface of the object is not representative of the bulk composition, then it is possible that surface-level XRF results may well be erroneously applied to the object as a

whole. For reference, based on the Beer-Lambert law, in a pure gold matrix, we would expect the beam intensity of the 9.71 keV L-Alpha secondary X-ray produced by gold to drop to c. 40% of its original intensity after c. 4 microns. For the 11.44 keV L-Beta secondary X-ray, it is c. 6 microns. As such, the vast majority of the secondary X-rays reaching the XRF detector will be originating from the first < 10 microns of the gold matrix analysed.

During the XRF analyses, two certified alloy standards were used. These were supplied by Micro-Analysis Consultants Ltd. and are referred to as MAC 1 and 2. Each standard was analysed a minimum of 72 times across the duration of the analyses. The XRF unit was accurate when analysing MAC 1 (94% Au, 4.5% Ag, 1% Cu) and MAC 2 (75% Au, 19% Ag, 5% Cu) — the results were within a fraction of 1 wt% for gold, silver and copper for both of these standards. None of the surfaces of the coins analysed were less than 82% gold.

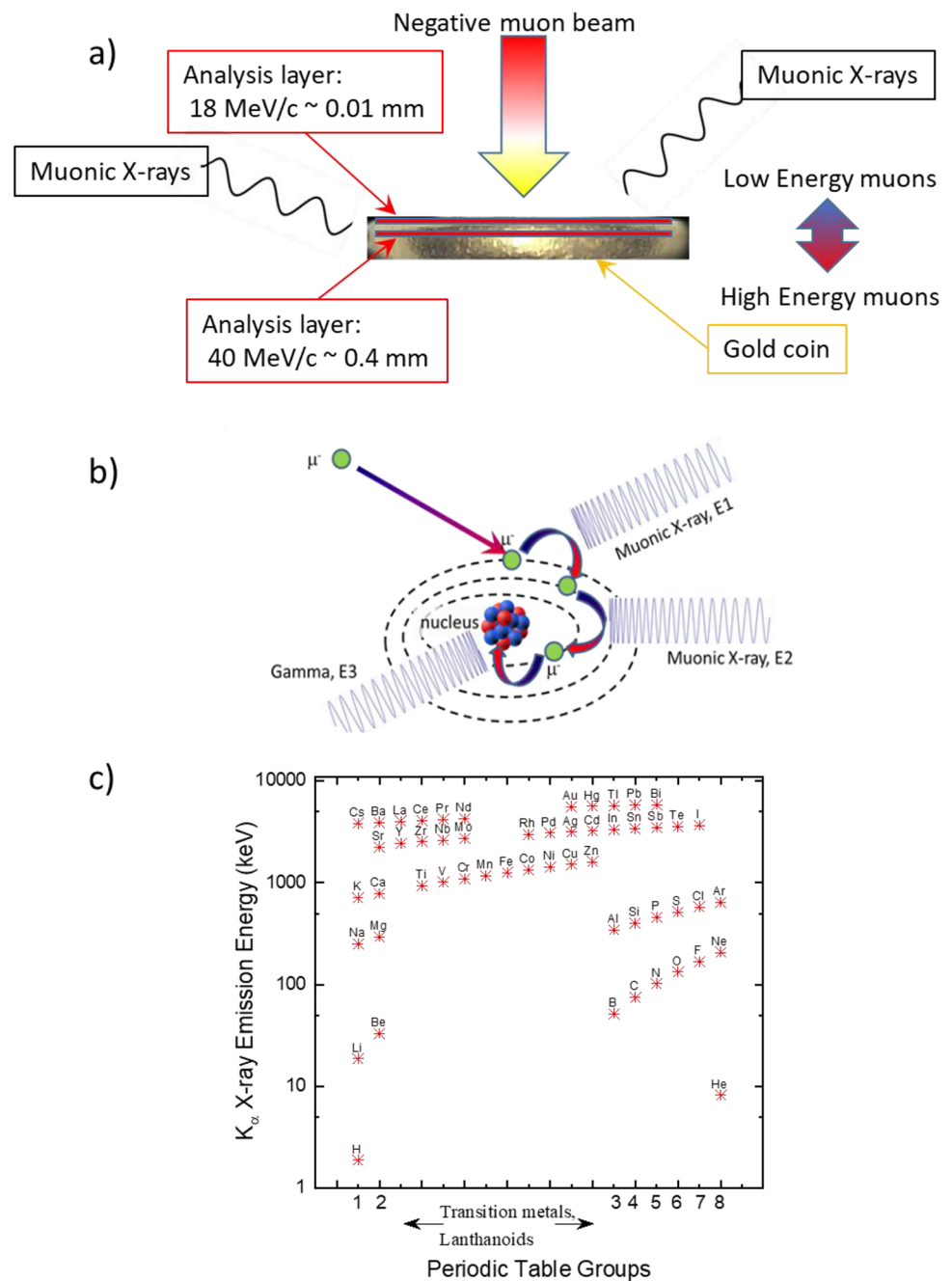
The XRF results for MAC 1 and 2 are accurate and consistent. For MAC 1, the largest absolute error for gold was 0.28 percentage points (*p.p.*), and the mean absolute error was 0.14 *p.p.* For silver, the largest absolute error was 0.16 *p.p.* and the mean absolute error was 0.06 *p.p.* For copper, the largest absolute error was 0.09 *p.p.* and the mean absolute error was 0.03 *p.p.* For MAC 2, the largest absolute error for gold was 0.61 *p.p.*, and the mean absolute error was 0.33 *p.p.* For silver, the largest absolute error was 0.45 *p.p.* and the mean absolute error was 0.20 *p.p.* For copper, the largest absolute error was 0.25 *p.p.* and the mean absolute error was 0.10 *p.p.* Given all this, the margin of error for the XRF results from the gold coins analysed here is probably significantly less than one percentage point. The full results of all the XRF analyses of the MAC standards can be found in the supplementary material.

The mean 2-sigma precision for all the gold measurements — standards and coins — ranged from ±0.10 to 0.11, for silver ranged from ±0.01 to 0.04 and for copper ranged from ±0.01 to 0.02.

Muonic X-ray emission spectroscopy

The muon experiments (data DOI: <https://doi.org/10.5286/ISIS.E.RB1920716>) were conducted at the RIKEN-RAL muon beamlines at the ISIS Pulsed Neutron and Muon Facility, STFC Rutherford Appleton Laboratory, UK (Matsuzaki et al. 2001; Hillier et al. 2019a; Thomason 2019). The negative muons are extracted from a carbon target that is bombarded with high energy protons. This creates pions which are extracted and decay into muons. These muons are momentum selected, which

Fig. 2 **a** A schematic of the implantation process for two muon energies. The higher energy muons are implanted at a deeper depth than the lower energy muons. This is confirmed in Fig. 3 which shows the implantation depth profile for the two energies used in this experiment. **b** A schematic of the capture process of the muon by an atom to form a muonic atom. The emissions are also shown from the cascade and capture processes. **c** The muonic X-ray emission energy for the $K\alpha$ transitions. All elements above and including Li can be observed. It is worth noting the y-axis is on a log scale, so it is evidently clear that elements next to each other are easily distinguishable

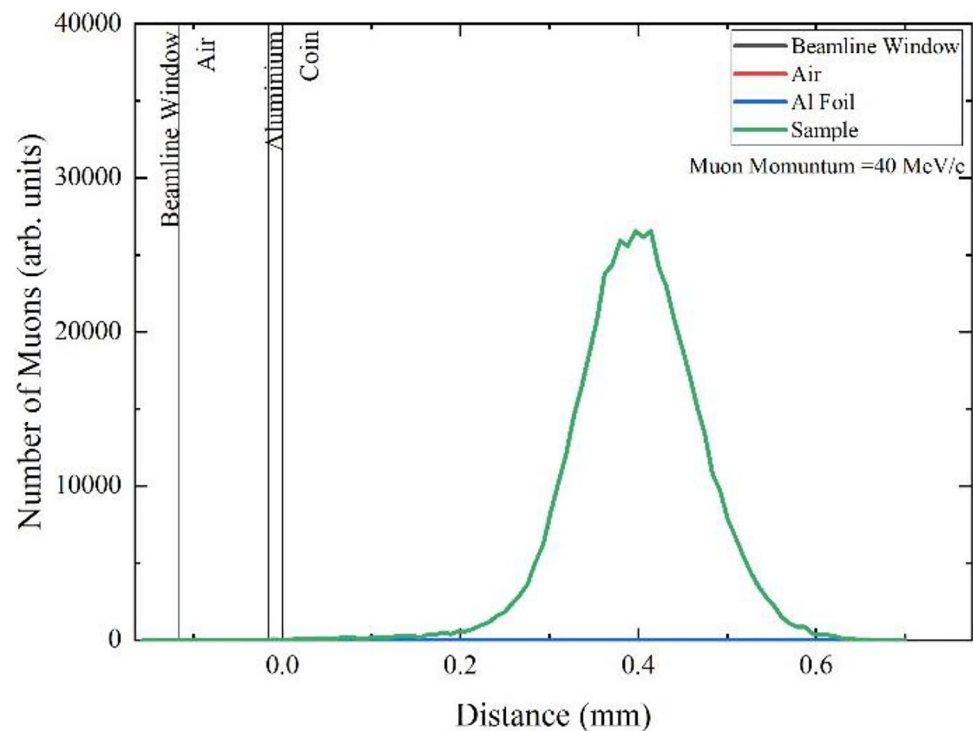


can be from 15 MeV/c up to, currently, 90 MeV/c with a momentum spread of 10% full width at half maximum (FWHM). This enables a layered compositional analysis of any material to be determined by simply controlling the momentum of the muons, i.e. sampling a thin layer within the material of interest. For pure gold, the implantation depth can be controlled between 10s of nanometres and 10s of millimetres. For our experiment, 40 MeV/c was used. The penetration depth of the 40 MeV/c muons was approximately 0.4 mm

(Figs. 2a and 3). The stopping profiles were calculated using SRIM/TRIM (Ziegler et al. 2010). This meant that our 40 MeV/c 'core' analyses penetrated approximately 30–45% of the way through the c. 1 mm thick coins analysed. The diameter of the muon beam can be varied from ~30 to 8 mm. For our experiment, the beam was centred on the portraits on the faces of the coins and illuminated the complete cross-section.

Once the negative muons are implanted, at a known depth, they are captured by the constituent atomic

Fig. 3 The calculated depth profiles of the negative muons at 40 MeV/c. At 40 MeV/c, the results show the implantation depth is c. 0.4 mm



elements and form a ‘muonic’ atom. These negative muons are initially captured, by energy transfer to the Auger electrons, in a high energy electronic state ($n \sim 14$) and then cascade down to the lowest state ($n = 1$). This happens in approximately 10^{-13} s. Each cascade results in the emission of an X-ray, whose energy is dependent upon the capturing atom (Fig. 2b). While a similar process to XRF, the mass of the muon is approximately 207 times that of an electron and results in these muonic X-rays being in the range of 10s keV to MeV (Fig. 2c)

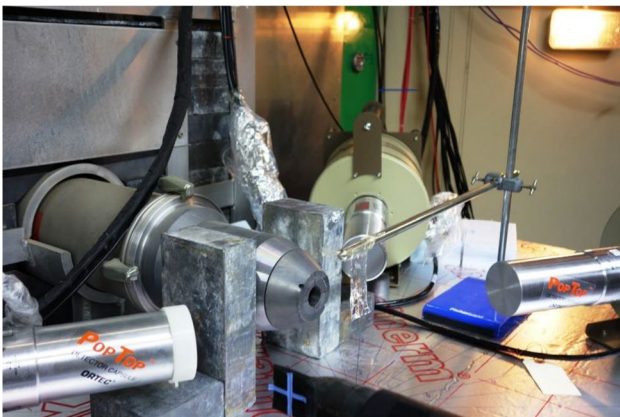


Fig. 4 A photo of the experimental setup for measuring the composition of a sample by muonic X-rays. The sample can be found in the aluminium packet held in front of the muon beam. Three of the four HPGe detectors are shown

(Measday 2001). As such, this results in self-absorption being much less of an issue and enables compositional analysis significantly beneath the surface. Finally, the muon will decay into an electron and a neutrino, or will be captured by the nucleus. If the muon is captured, then a muon and proton reaction can take place and a gamma can be emitted (along with a neutron). The gamma emission can potentially give isotope analysis (Ninomiya 2018). All of these emissions are in the order of 10s keV up to approximately 8 MeV and can be detected by high-purity germanium detectors.

The experimental setup comprises of four ORTEC high-purity germanium detectors (HPGe), two upstream and two downstream, running the EXP2K software (Nakamura and Iwasaki 1997). Each pair of detectors consists of low-energy high-resolution detector (30 keV–1 MeV) and a high-energy lower-resolution detector (50 keV–8 MeV). The coins were mounted in an aluminium package, with one covering 0.016 mm thickness. An image of the experimental setup can be seen in Fig. 4, and a fuller description can be found in Hampshire et al. (Hampshire et al. 2019) and Hillier et al. (Hillier et al. 2016). For an introductory overview of the technique, see Hillier et al. (Hillier et al. 2021), and for a more technical description, see Measday (Measday 2001).

Now concentrating on the details for our experiment, in order to make the identification of the muonic X-rays easier, elements (purity > 99.9%) of the expected significant

Fig. 5 The data and the fits for the MAC gold standards. Each clearly showing a change in the peak intensity dependent upon the composition. The red line is the fit to the data and the vertical lines show the important Au, Ag and Cu peaks (in gold, grey and orange, respectively)

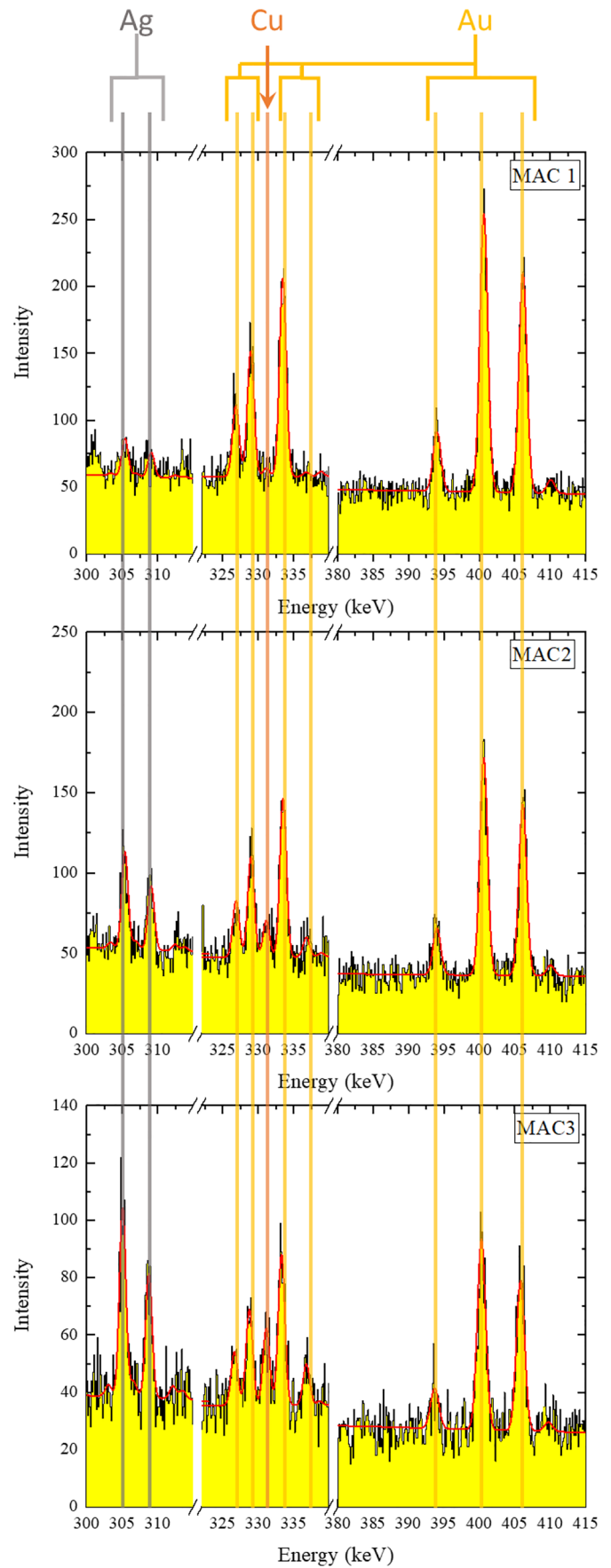
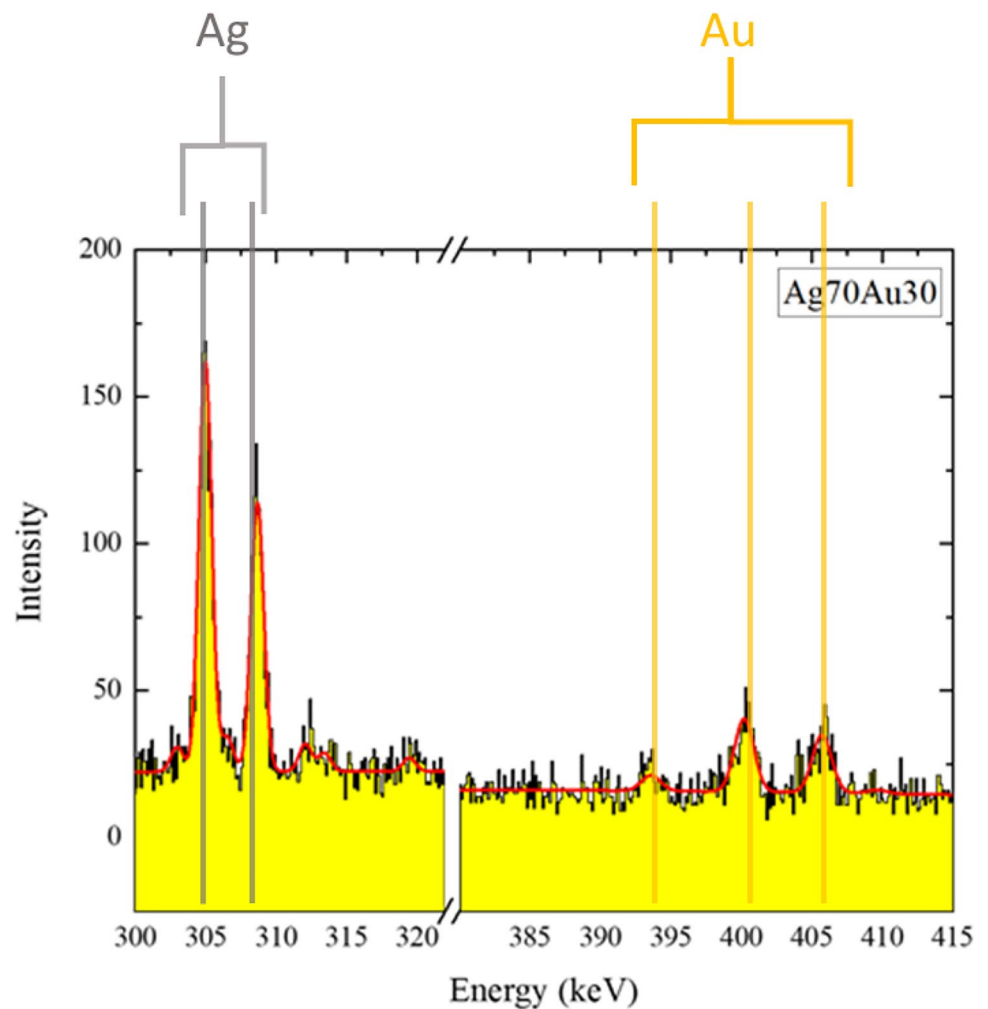


Fig. 6 The data and fits for the Ag70Au30 sample. The red line is the fit to the data and the vertical lines show the important Ag and Au peaks (in grey and gold, respectively)



constituent components were analysed. In this case: gold, silver and copper. The identification of elements in the gold coins was conducted using the peak parameters from the pure elements and then varying the silver to gold ratio. The MAC standards used in the XRF measurements were also measured and were used to calibrate the experimental setup, along with a silver/gold mixture (70:30), pure silver and pure gold (Hillier et al. 2019b; Hillier et al. 2015). The spectra from these gold reference materials can be viewed in Figs. 5 and 6. The energy spectra from the muonic X-ray emission were collected from 10s of keV up to 8 MeV. These figures

show gold (Au) peaks around 400 keV; silver (Ag) peaks at 305 and 310 keV; and a copper (Cu) peak at 330 keV. The peak intensities show a change in intensities that is proportional to the composition of each standard. The peak intensities for each standard are shown in Table 2. These measurements, alongside the statistics collected, show that the minimum composition detectable was approximately 1%. Future detector and instrument improvements should be able to further reduce this. Examples of the μ XES spectra produced by a pure and heavily debased gold coin can be viewed in Figs. 7 and 8.

Table 2 The results of the relative peak intensity of gold, silver and copper from the gold alloy standards analysed. The uncertainty of the measurement is located in the adjacent brackets. Please note that

the presence of 0.5% and 1% tin in MAC 1 and 2 respectively have caused elevated silver intensities and depressed copper intensities — this phenomenon does not occur in the coins analysed

Standard	Gold peak intensity (%)	Silver peak intensity (%)	Copper peak intensity (%)
MAC 1 (94Au, 4.5Ag, 1Cu)	93.9 (± 0.6)	5.2 (± 0.6)	0.94 (± 0.6)
MAC 2 (75Au, 19Ag, 5Cu)	75.0 (± 0.7)	21.0 (± 0.8)	4.0 (± 0.8)
Ag ₇₀ Au ₃₀ (30Au, 70Ag)	33 (± 1)	67 (± 1)	n/a

Fig. 7 The μ XES spectra and fits from coin #14 — the full purity RIC2 9 type of Otho. Note the lack of silver peaks at 305 keV and 310 keV, and the lack of copper peak at c. 330 keV

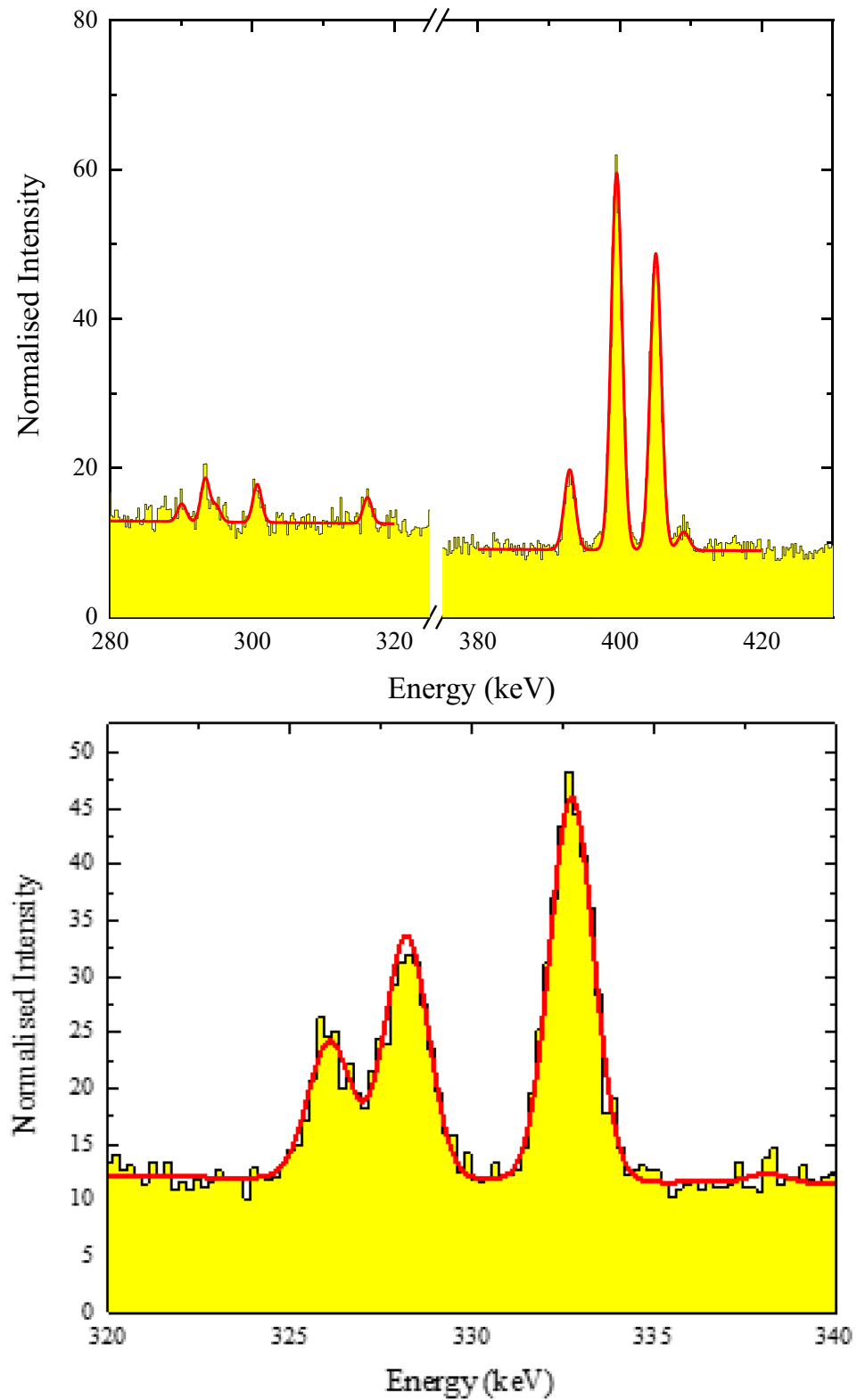
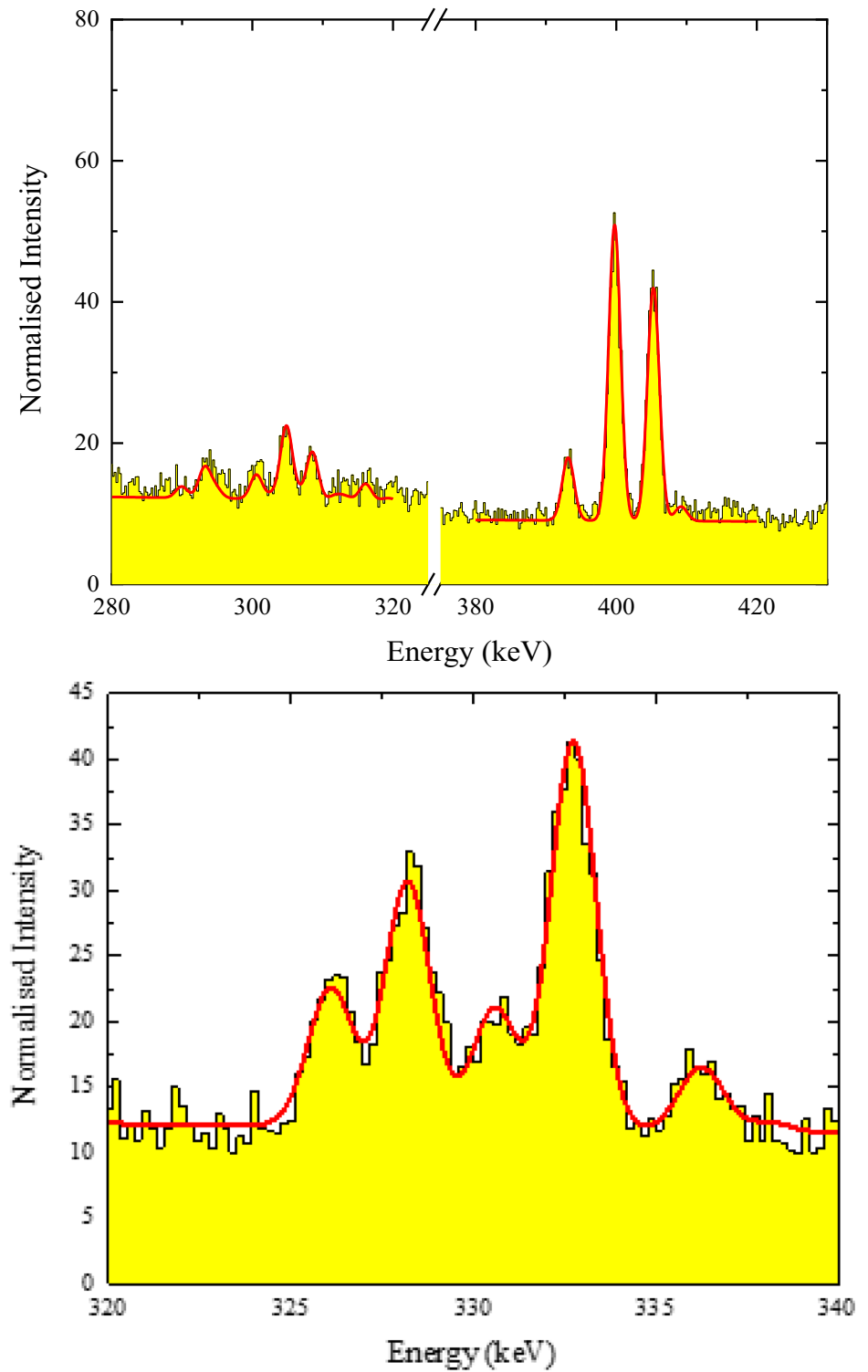


Fig. 8 The μ XES spectra and fits from coin #16 — the heavily debased RIC2 9 type of Otho. Note the silver peaks at 305 keV and 310 keV, and the copper peak at c. 330 keV



Supplementary Information The online version contains supplementary material available at <https://doi.org/10.1007/s12520-022-01631-1>.

Author contribution G.A.G.: conceptualisation, methodology, validation, formal analysis, investigation, resources, writing — original draft, visualisation, project administration, funding acquisition.

T.A.: conceptualisation, methodology (μXES), validation (μXES), formal analysis (μXES), investigation (μXES), writing — review and editing.

K.D.: conceptualisation, methodology (XRF), validation (XRF), investigation (XRF), writing — review and editing.

A.D.H.: conceptualisation, methodology (μXES), validation (μXES), formal analysis (μXES), investigation (μXES), resources, writing — original draft, project administration (μXES), funding acquisition.

K.I.: conceptualisation, methodology (μXES), validation (μXES), formal analysis (μXES), investigation (μXES), writing — review and editing, project administration (μXES), funding acquisition.

Funding The lead author received initial ‘pump-priming’ funding from the University of Oxford’s John Fell Fund. The lead author is currently supported by a Leverhulme Trust Early Career Fellowship grant (ECF-2020-211). This project received muon beam time from the ISIS Neutron and Muon Source.

Data availability Data supporting the findings of this study are available within the article and in the [supplementary material](#).

Declarations

Conflict of interest The authors declare no competing interests.

Open Access This article is licensed under a Creative Commons Attribution 4.0 International License, which permits use, sharing, adaptation, distribution and reproduction in any medium or format, as long as you give appropriate credit to the original author(s) and the source, provide a link to the Creative Commons licence, and indicate if changes were made. The images or other third party material in this article are included in the article's Creative Commons licence, unless indicated otherwise in a credit line to the material. If material is not included in the article's Creative Commons licence and your intended use is not permitted by statutory regulation or exceeds the permitted use, you will need to obtain permission directly from the copyright holder. To view a copy of this licence, visit <http://creativecommons.org/licenses/by/4.0/>.

References

- Bachman H-G (1995) Sophisticated Roman recovery. *Tech Gold Inst Archaeo-Metall Stud Newsl* 19:7–9
- Baker J et al (2018) The reformed Byzantine silver based currencies (ca. 1372–1379) in the light of the hoards from the Belgrade Gate. *Dumbarton Oaks Pap* 71:273–335
- Blakelock ES (2016) Never judge a gold object by its surface analysis: a study of surface phenomena in a selection of gold objects from the Staffordshire Hoard. *Archaeometry* 58:912–929
- Blet-Lemarquand M, Suspène A, Amandry M (2015) In: Hauptmann A, Modarressi-Tehrani D (Eds) *Archaeometallurgy in Europe III Proceedings of the 3rd International Conference Deutsches Bergbau-Museum Bochum June 29 – July 1, 2011*. Deutsches Bergbau-Museum, p 107–113
- Blet-Lemarquand M, Nieto-Pelletier S, Téreygeol F, Suspène (2017) In: Montero Ruiz I, Perea A (Eds) *Archaeometallurgy in Europe IV. Consejo Superior de Investigaciones Científicas*, p 19–28
- Bocciarelli D, Blet-Lemarquand M, Suspène A (2017) In: Bricault L, Burnett A, Drost V, Suspène A (eds) *Rome et les Provinces. Monnayage et Histoire. Mélanges offerts à Michel Amandry*, Bordeaux, Ausonius éditions, pp 175–188
- Butcher K, Ponting M, Evans J, Pashley V, Somerfield C (2014) *The metallurgy of Roman silver coinage: from the reform of Nero to the reform of Trajan*. Cambridge University Press
- Caley ER (1952) Estimation of composition of ancient metal objects. *Anal Chem* 24:676–681
- Callu JP, Brenot C, Barrandon N, Poirier J (1985) In: Morrisson C (eds) *L’Or monnayé I. Purification et altérations de Rome à Byzance*. Centre National de la Recherche Scientifique, p 81–111
- Cowell MR (1998) In: Oddy WA, Cowell MR (eds) *Metallurgy in Numismatics, Vol. 4*. Royal Numismatic Society, p 448–460
- Geil EC, Thorne RE (2014) Correcting for surface topography in X-ray fluorescence imaging. *J Synchrotron Radiat* 21:1358–1363
- Green GA et al (2021) Understanding Roman gold coinage inside out. *J Archaeol Sci* 134:105470. <https://doi.org/10.1016/j.jas.2021.105470>
- Guerra MF, Calligaro T (2004) Gold traces to trace gold. *J Archaeol Sci* 31:1199–1208
- Hall ET (1961) Surface enrichment of buried metals. *Archaeometry* 4:61–66
- Hampshire B et al (2019) Using negative muons as a probe for depth profiling silver Roman coinage. *Heritage* 2:400–407
- Healy JF (1979) Mining and processing gold ores in the ancient world. *J Met* 11–16
- Hillier AD et al (2015) Using negative muons as a non-destructive probe of material composition. *STFC ISIS Neutron and Muon Source*. <https://doi.org/10.5286/ISIS.E.RB1510343>
- Hillier AD, Paul D, Ishida K (2016) Probing beneath the surface without a scratch — bulk non-destructive elemental analysis using negative muons. *Microchem J* 125:203–207. <https://doi.org/10.1016/j.microc.2015.11.031>
- Hillier AD, Lord JS, Ishida K, Rogers C (2019) Muons at ISIS. *Philosophical Transact R Soc a: Math, Phys Eng Sci* 377:20180064. <https://doi.org/10.1098/rsta.2018.0064>
- Hillier AD et al (2019) How low can you go? *STFC ISIS Neutron and Muon Source*. <https://doi.org/10.5286/ISIS.E.RB1820616-1>
- Hillier A, Hampshire B, Ishida K (2021) In: D’Amico S, Venuti V (eds) *Handbook of cultural heritage analysis*. Springer Nature Switzerland AG
- Karydas AG (2007) Application of a portable XRF spectrometer for the non-invasive analysis of museum metal artefacts. *Anal Chim* 97:419–432
- Matsuzaki T et al (2001) The RIKEN-RAL pulsed muon facility. *Nucl Instrum Methods Phys Res, Sect A* 465:365–383. [https://doi.org/10.1016/S0168-9002\(01\)00694-5](https://doi.org/10.1016/S0168-9002(01)00694-5)
- Measday DF (2001) The nuclear physics of muon capture. *Phys Rep* 354:243–409. [https://doi.org/10.1016/S0370-1573\(01\)00012-6](https://doi.org/10.1016/S0370-1573(01)00012-6)
- Nakamura SN, Iwasaki M (1997) A new data acquisition system for the RIKEN-RAL μCF experiment. *Nucl Instrum Methods Phys Res, Sect A* 388:220–225. [https://doi.org/10.1016/S0168-9002\(97\)00343-4](https://doi.org/10.1016/S0168-9002(97)00343-4)
- Ninomiya K et al (2015) Nondestructive elemental depth-profiling analysis by muonic X-ray measurement. *Anal Chem* 87:4597–4600. <https://doi.org/10.1021/acs.analchem.5b01169>
- Ninomiya K et al (2018) in *Proceedings of the 14th International Conference on Muon Spin Rotation, Relaxation and Resonance (?SR2017)*, Vol. 21 JPS Conference Proceedings. *J Phy Soc Japan*
- Notton JHF (1974) Ancient Egyptian gold refining. *Gold Bulletin* 7:50–56
- Oddy WA (1986) The touchstone: the oldest colorimetric method of analysis. *Endeavour* 10:164–166
- Ogden J (2000) In: Nicholson PT (eds) *Shaw I Ancient Egyptian materials and technology*. Cambridge University Press, p 148–177

- Raub CJ (1995) In: Morteani G, Northover JP (eds) Prehistoric Gold in Europe. Kluwer Academic Publishers, p 243–260
- Simsek Franci G (2020) Handheld X-ray fluorescence (XRF) versus wavelength dispersive XRF: characterization of Chinese blue-and-white porcelain sherds using handheld and laboratory-type XRF instruments. *Appl Spectrosc* 74:314–322
- Tanaka R, Yuge K, Kawai J, Alawadhi H (2017) Artificial peaks in energy dispersive X-ray spectra: sum peaks, escape peaks, and diffraction peaks: artificial peaks in energy dispersive X-ray spectra. *X-Ray Spectrom* 46:5–11
- Thomason JWG (2019) The ISIS spallation neutron and muon source—the first thirty-three years. *Nucl Instrum Methods Phys Res, Sect A* 917:61–67. <https://doi.org/10.1016/j.nima.2018.11.129>
- Van Grieken R, Markowicz A (2001) Handbook of X-ray spectrometry. 2nd edn, Marcel Dekker, Inc
- Ziegler JF, Ziegler MD, Biersack JP (2010) SRIM — the stopping and range of ions in matter. *Nucl instrum methods phys res Sect B, Beam interact mater atoms* 268:1818–1823

Publisher's note Springer Nature remains neutral with regard to jurisdictional claims in published maps and institutional affiliations.